On the output factor measurements of the CyberKnife iris collimator small fields: Experimental determination of the $k^{f_{clin},f_{msr}}_{Q_{clin},Q_{msr}}$ correction factors for microchamber and diode detectors

E. Pantelis[a)]
Medical Physics Laboratory, Medical School, University of Athens, 75 Mikras Asias, 115 27 Athens, Greece and CyberKnife Center, Iatropolis-MagnitikiTomografia, 54-56 Ethnikis-Antistaseos, 152 31 Athens, Greece

A. Moutsatsos and K. Zourari
Medical Physics Laboratory, Medical School, University of Athens, 75 Mikras Asias, 115 27 Athen, Greece

L. Petrokokkinos and L. Sakelliou
Nuclear and Particle Physics Section, Physics Department, University of Athens, Panepistimioupolis, Ilisia, 157 71 Athens, Greece

W. Kilby
Accuray Incorporated, Sunnyvale, California 94089

C. Antypas
1st Department of Radiology, Aretaieion Hospital, Medical School, University of Athens, Vas. Sophias, 115 28 Athens, Greece and CyberKnife Center, Iatropolis-MagnitikiTomografia, 54-56 Ethnikis-Antistaseos, 152 31 Athens, Greece

P. Papagiannis, P. Karaiskos, and E. Georgiou
Medical Physics Laboratory, Medical School, University of Athens, 75 Mikras Asias, 115 27 Athens, Greece

I. Seimenis
Medical Physics Laboratory, Medical School, Democritus University of Thrace, 2nd Building of Preclinical Section, University Campus, 68100 Alexandroupolis, Greece

(Received 8 February 2012; revised 14 June 2012; accepted for publication 16 June 2012; published 20 July 2012)

Purpose: To measure the output factors (OFs) of the small fields formed by the variable aperture collimator system (iris) of a CyberKnife (CK) robotic radiosurgery system, and determine the $k^{f_{clin},f_{msr}}_{Q_{clin},Q_{msr}}$ correction factors for a microchamber and four diode detectors.
Methods: OF measurements were performed using a PTW PinPoint 31014 microchamber, four diode detectors (PTW-60017, −60012, −60008, and the SunNuclear EDGE detector), TLD-100 microcubes, alanine dosimeters, EBT films, and polymer gels for the 5 mm, 7.5 mm, 10 mm, 12.5 mm, and 15 mm iris collimators at 650 mm, 800 mm, and 1000 mm source to detector distance (SDD). The alanine OF measurements were corrected for volume averaging effects using the 3D dose distributions registered in polymer gel dosimeters. $k^{f_{clin},f_{msr}}_{Q_{clin},Q_{msr}}$ correction factors for the PinPoint microchamber and the diode dosimeters were calculated through comparison against corresponding polymer gel, EBT, alanine, and TLD results.
Results: Experimental OF results are presented for the array of dosimetric systems used. The PinPoint microchamber was found to underestimate small field OFs, and a $k^{f_{clin},f_{msr}}_{Q_{clin},Q_{msr}}$ correction factor ranging from 1.127 ± 0.022 (for the 5 mm iris collimator) to 1.004 ± 0.010 (for the 15 mm iris collimator) was determined at the reference SDD of 800 mm. The PinPoint $k^{f_{clin},f_{msr}}_{Q_{clin},Q_{msr}}$ correction factor was also found to increase with decreasing SDD; $k^{f_{clin},f_{msr}}_{Q_{clin},Q_{msr}}$ values equal to 1.220 ± 0.028 and 1.077 ± 0.016 were obtained for the 5 mm iris collimator at 650 mm and 1000 mm SDD, respectively. On the contrary, diode detectors were found to overestimate small field OFs and a correction factor equal to 0.973 ± 0.006, 0.954 ± 0.006, 0.937 ± 0.007, and 0.964 ± 0.006 was measured for the PTW-60017, −60012, −60008 and the EDGE diode detectors, respectively, for the 5 mm iris collimator at 800 mm SDD. The corresponding correction factors for the 15 mm iris collimator were found equal to 0.997 ± 0.010, 0.994 ± 0.009, 0.988 ± 0.010, and 0.986 ± 0.010, respectively. No correlation of the diode $k^{f_{clin},f_{msr}}_{Q_{clin},Q_{msr}}$ correction factors with SDD was observed.
Conclusions: This work demonstrates an experimental procedure for the determination of the $k^{f_{clin},f_{msr}}_{Q_{clin},Q_{msr}}$ correction factors required to obtain small field OF results of increased accuracy.
 [http://dx.doi.org/10.1118/1.4736810]

Key words: small fields, output factor, correction factor, polymer gel, CyberKnife

I. INTRODUCTION

Small photon fields formed by circular collimators or multileaf collimators (MLCs) are routinely used for stereotactic radiosurgery/radiotherapy and intensity modulated radiation therapy (IMRT). Experimental dosimetry of such radiation fields remains one of the most challenging tasks to perform, mainly, due to the combined effect of steep dose gradients and loss of lateral electronic equilibrium.[1–10] While percentage depth dose curves and relative off axis profiles obtained using different detectors do not present significant differences,[5,8,10,11] relative output factor (OF) measurements are characterized by a considerable interdetector variations which, in principle, increases with decreasing field size.[1,7–10,12] The observed variations are not only attributed to the specific drawbacks of the different dosimetry systems used,[3–5,7–9,12–14] but also to volume averaging effects,[7,14,15] detector positioning,[16] and the presence of the detector, which perturbs the local level of disequilibrium.[17]

A recently published dosimetric formalism suggests the use of appropriate correction factors, $\boldsymbol{k}_{Q_{\text{clin}},Q_{\text{msr}}}^{f_{\text{clin}},f_{\text{msr}}}$, in order to increase the accuracy of small and nonstandard field OF measurements using different types of dosimetric systems.[18] These correction factors are not only machine and detector specific, but also depend on beam energy and field size. This renders their accurate determination a nontrivial task,[12,13,18] and experimental methods, alone or combined with detector response function convolution techniques, and Monte Carlo (MC) simulation have been used.[12–14,18–21] While MC simulation is gaining wide acceptance for estimating the dosimetric properties of small and nonstandard fields, mainly, due to the limited type A (statistical) uncertainty of corresponding results,[12–14,19,20] experimental validation is still required to rule out the potential influence of type B (systematic) uncertainties associated with the particle transport characteristics (e.g., cross section libraries, particle transport algorithm limitations), as well as with detector and radiation geometry modelling.[19,22–25]

The CyberKnife® (CK) Robotic Radiosurgery System (Accuray Incorporated, Sunnyvale, USA) employs a single modality linear accelerator to generate a 6MV x-ray treatment beam.[26] The beam is collimated using a set of 12 fixed circular collimators to form field sizes ranging from 5 mm to 60 mm nominal diameter at 800 mm from the x-ray source.[26,27] For this system, a machine specific MC based technique has been proposed for the calculation of $\boldsymbol{k}_{Q_{\text{clin}},Q_{\text{msr}}}^{f_{\text{clin}},f_{\text{msr}}}$ correction factors for OF measurements of the fixed collimators, using a variety of dosimetric systems.[12,13] The specific methodology has been independently verified through comparison of corrected OF values measured using microchambers and diode detectors with corresponding results obtained using small TLD-100 microcubes, alanine dosimeters, EBT films, and polymer gels.[14]

Recently, the CK system has been equipped with the Iris™ variable aperture collimator, which creates circular fields with the same nominal diameters as those of the fixed collimators.[26] While off axis profiles of the new variable aperture collimation system are generally in close agreement with corresponding fixed collimator field profiles,[28] the OFs measured for the iris small fields are relatively lower. This has been attributed to the increased length of the iris collimator and the difference in the head scatter component.[28]

In this work, the OFs for the iris fields of 5 mm, 7.5 mm, 10 mm, 12.5 mm, and 15 mm nominal diameter were measured using a multitude of dosimetric systems including a microchamber, four diode detectors, TLD-100 microcubes, alanine dosimeters, EBT Gafchromic films, and polymer gels. Measurements were performed at 650 mm, 800 mm and 1000 mm source to detector distance (SDD) as necessitated by the commissioning of the MultiPlan® treatment planning system. OF results from polymer gel, EBT film, alanine, and TLD measurements were used for the experimental determination of the $\boldsymbol{k}_{Q_{\text{clin}},Q_{\text{msr}}}^{f_{\text{clin}},f_{\text{msr}}}$ correction factors for the microchamber and diode detectors.

II. MATERIALS AND METHODS

The OF, $\boldsymbol{k}_{Q_{\text{clin}},Q_{\text{msr}}}^{f_{\text{clin}},f_{\text{msr}}}$, of a CK clinical field, f_{clin}, is defined as

$$\Omega_{Q_{\text{clin}},Q_{\text{msr}}}^{f_{\text{clin}},f_{\text{msr}}} = \frac{\dot{D}^{f_{\text{clin}}}(r = 0\text{ mm}, \text{SDD})}{\dot{D}^{f_{\text{msr}}}(r = 0\text{ mm}, \text{SDD} = 800\text{ mm})}\left(\frac{\text{SDD}}{800}\right)^2, \quad (1)$$

where, $\dot{D}^{f_{\text{clin}}}(r = 0\text{ mm}, \text{SDD})$ and $\dot{D}^{f_{\text{msr}}}(r = 0\text{ mm}, \text{SDD} = 800\text{ mm})$ stand for the dose at 15 mm depth in water per monitor unit (MU) at the center ($r = 0$ mm) of the f_{clin} and the machine specific reference (msr) field, f_{msr}, respectively. The msr field is defined as the 60 mm diameter field at the 800 mm reference SDD using the fixed collimation system. The CK system, however, is nonisocentric and treatment is routinely performed at SDDs other than 800 mm. OFs determined at 650 mm, 800 mm, and 1000 mm SDD are therefore imported to the treatment planning system and used in combination with the inverse square law to model the output variation with distance. It is noted that in CK practice, the available clinical field sizes are reported as *collimator sizes* determined by the nominal field diameter at 800 mm SDD. According to this terminology, however, the reported 5 mm collimator size corresponds to a projected field diameter (f_{clin}) of 4.1 mm, 5 mm, and 6.3 mm at 650 mm, 800 mm, and 1000 mm SDD, respectively. To avoid confusion between collimator size and projected field size henceforth, f_{clin} will be reported by stating the corresponding collimator size along with the measurement SDD following the aforementioned terminology.

To increase OF measurement accuracy, Alfonso *et al.*[18] suggested $\Omega_{Q_{\text{clin}},Q_{\text{msr}}}^{f_{\text{clin}},f_{\text{msr}}}$ to be calculated as the ratio of detector readings, $M_{Q_{\text{clin}}}^{f_{\text{clin}}}$ and $M_{Q_{\text{msr}}}^{f_{\text{msr}}}$, at f_{clin} and f_{msr}, respectively, multiplied by a $k_{Q_{\text{clin}},Q_{\text{msr}}}^{f_{\text{clin}},f_{\text{msr}}}$ correction factor according to

$$\Omega_{Q_{\text{clin}},Q_{\text{msr}}}^{f_{\text{clin}},f_{\text{msr}}} = \frac{M_{Q_{\text{clin}}}^{f_{\text{clin}}}}{M_{Q_{\text{msr}}}^{f_{\text{msr}}}} * k_{Q_{\text{clin}},Q_{\text{msr}}}^{f_{\text{clin}},f_{\text{msr}}}. \quad (2)$$

For detectors with $\boldsymbol{k}_{Q_{\text{clin}},Q_{\text{msr}}}^{f_{\text{clin}},f_{\text{msr}}}$ equal to unity, the ratio of the detector readings (to be referred to in the following as measured or uncorrected OF) coincides with $\Omega_{Q_{\text{clin}},Q_{\text{msr}}}^{f_{\text{clin}},f_{\text{msr}}}$.

Results obtained by such detectors can be used to compile a $\Omega_{Q_{\mathrm{clin}},Q_{\mathrm{msr}}}^{f_{\mathrm{clin}},f_{\mathrm{msr}}}$ dataset useful for the experimental determination of $\boldsymbol{k}_{Q_{\mathrm{clin}},Q_{\mathrm{msr}}}^{f_{\mathrm{clin}},f_{\mathrm{msr}}}$ correction factors for other detectors, provided that they are characterized by increased accuracy. In this work, the error weighted average[29] of OF measured by alanine, TLD, EBT film, and polymer gel dosimeters (for which $k_{Q_{\mathrm{clin}},Q_{\mathrm{msr}}}^{f_{\mathrm{clin}},f_{\mathrm{msr}}} = 1$)[14] were used for the experimental determination of microchamber and diode detectors $\boldsymbol{k}_{Q_{\mathrm{clin}},Q_{\mathrm{msr}}}^{f_{\mathrm{clin}},f_{\mathrm{msr}}}$ correction factors for the small iris fields of the CK system.

II.A. Chamber and diode measurements

The PinPoint 31014 microchamber (PTW, Freiburg, Germany), the recently introduced PTW-60017 *p*-type unshielded diode and its predecessor PTW-60012, the PTW-60008 *p*-type shielded diode, as well as the copper shielded *n*-type EDGE detector (SunNuclear Corp., Florida, USA) were used. All detectors were placed with their stem parallel to the beam axis except for the EDGE detector. Considering its design, the EDGE detector was positioned with its stem perpendicular to the beam axis to achieve an active layer alignment equivalent to that of the other diode detectors. Precise alignment of the detector with the beam axis is of increased importance for low uncertainty small field dosimetry.[14,16] Orthogonal off axis profiles were therefore acquired prior to measurements with each detector to align its reference point of measurement with the beam center. The reference point lay at the depth of the active layer for the diode detectors (i.e., 0.8 mm, 0.6 mm, 2.0 mm, and 0.3 mm, for the PTW 60017, −60012, −60008, and EDGE diodes, respectively), and 3.7 mm from its external tip for the PinPoint microchamber.[12] Measurements were performed for the field sizes formed by the 5 mm, 7.5 mm, 10 mm, 12.5 mm, and 15 mm iris collimators at 650 mm, 800 mm, and 1000 mm SDD, as well as for the 60 mm msr field. 100 MUs were delivered to the reference point of each detector placed at 15 mm depth in water, except for the PTW-60017 where 200 MUs were delivered given its relatively lower sensitivity. Measurements were repeated at least five times (ten times for the two smaller fields) with the iris collimator instructed to fully open and re-establish the measured field in between measurements. For the PinPoint microchamber measurements were performed with both positive and negative polarity (± 400 V) and averaged since a polarity effect of magnitude varying with field size and SDD was observed (±4.4%, ±3.6%, and ±2.4% with respect to the average for the 5 mm collimator at 650 mm, 800 mm, and 1000 mm SDD, respectively). Charge was collected using a PTW-UNIDOS electrometer.

The uncertainty associated with the OF results of this work was estimated following the recommendations of the Guide to the Expression of Uncertainty in Measurement.[30] The type A uncertainty component, estimated from repeated measurements, characterizes the precision of MU delivery, charge collection, and measured field formation by the iris collimator.[28] The type B uncertainty component was calculated[31] taking into account the ± 0.5 mm, ± 0.2 mm, and ± 0.2 mm uncertainties in determining the SSD, positioning the reference point of measurement at 15 mm depth, and aligning the reference point of measurement with the beam axis, respectively, assuming rectangular distributions. The type B uncertainty associated with the polarity effect was also considered for PinPoint results.

II.B. Alanine and TLD measurements

Alanine pellets (cylindrically shaped with 2.5 mm height and 5 mm diameter) were provided by the therapy level alanine dosimetry service[32] of the National Physical Laboratory (NPL). TLD measurements were performed using LiF TLD type 100 microcubes of 1 × 1 × 1 mm^3 (Harshaw/Bicron, Solon, OH). The TLD microcubes were sorted, group-annealed (1 h at 400 °C, followed by 2 h at 100 °C) and subjected to prereadout annealing (10 min at 100 °C) after radiation exposure. TLD calibration was performed using a 100 × 100 mm^2 6 MV photon field and a Model 2800 M, Victoreen TLD system was used for signal readout.

Both types of dosimeters were irradiated with their reference point of measurement, assumed to coincide with their geometrical center, aligned with the radiation beam center at 15 mm depth inside a water phantom.[14] A nominal dose of 10 Gy and 1 Gy was delivered to each alanine pellet and TLD microcube, respectively. Repeated measurements were carried out as described in Sec. II.A for the same iris fields and SDDs. OFs were calculated as the ratio of the measured dose per MU of each clinical field normalized to the corresponding ratio for the 60 mm msr field according to Eq. (1).

The 5 mm diameter of the alanine pellet introduces a significant volume averaging effect to measurements of this work for all but the 60 mm diameter msr field. Appropriate correction factors were therefore calculated using corresponding gel dosimetry results (see Sec. II.D) and applied to the alanine measured OFs.

The uncertainty assigned to the TLD and alanine measured OFs was estimated as described in Sec. II.A. Type A uncertainty was estimated from error propagation on the standard deviation of the mean dose of the detectors irradiated for each field size, while type B uncertainty was estimated taking into account the uncertainties associated with the calibration procedure, the experimental setup, and the volume averaging correction factors for alanine pellets.

II.C. EBT film measurements

Gafchromic EBT-1 films (ISP, Wayne, NJ) were used following the data acquisition and processing protocol suggested by Devic *et al.*[33] Precut EBT films (Lot: 47277–03I) of 60 × 60 mm^2 size for the msr field and 20 × 20 mm^2 size for the iris small fields were placed at 15 mm depth in RW3 solid water slabs of 200 mm total thickness and 300 × 300 mm^2 in-plane dimensions. Repeated measurements were carried out as described in Sec. II.A for the same iris fields and SDDs. A nominal dose of 4 Gy was delivered to each film. All films were scanned one day postirradiation using a Microtek flatbed optical scanner operated in transmission mode. RGB images of 48-bit depth and 150 dpi resolution (pixel size

= 0.169 mm) were obtained, but only the red color channel of the image was used. A 3 × 3 Wiener low pass filter was applied prior to further processing to minimize noise. The symmetry of each circular radiation field as recorded on film was used to define the coordinates of its center.[8,14] The pixel values lying within a circle of appropriate diameter (0.5 mm, 1 mm, 2 mm, 3 mm, and 5 mm for the 5 mm and 7.5 mm, 10 mm, 12.5 mm, 15 mm and 60 mm collimators, respectively), centered at the corresponding radiation field center, were averaged and used to calculate the optical density (OD) of each film. The OD values of the films irradiated with the same field were averaged and converted to dose using the calibration curve for the film batch used in this work. OFs were calculated as the ratio of the measured dose per MU of each field normalized to the corresponding ratio for the 60 mm msr field according to Eq. (1). The uncertainty of the measured OFs was estimated using error propagation[30] on (a) the standard deviation of the average OD at the center of each field (type A) and (b) the type B uncertainty components associated with the calibration procedure and the establishment of the desired SSD. The type B uncertainty associated with the determination of the radiation field center on each film was found equal to $u_{center} = 0.02$ mm (calculated as the standard deviation of the mean of the coordinates of the center of mass of the 2D objects determined on each film using different OD threshold values)[8,14] and therefore excluded from consideration.

II.D. Polymer gel dosimetry measurements

The VIP polymer gel formulation was used for polymer gel measurements in this work.[8,34,35] Following preparation,[8,34,35] the gel was poured into three orthogonal PMMA containers (200 × 200 × 45 mm^3 external dimensions). The gel containers were hermetically sealed, transferred to the CK department, and left overnight to solidify. Irradiation was performed in the next two days; on the first day containers 1 and 3 were irradiated using the 650 mm and 800 mm SDDs, respectively, and on the second day container 2 was irradiated using the 1000 mm SDD. All irradiations were performed with the gel dosimeters inside a water phantom to establish full scatter conditions [see Figs. 1(a) and 1(b)]. Solid water slabs were also placed beneath each gel container to align its upper surface with the water surface [see Fig. 1(b)]. Twenty-nine radiation shots were delivered to each gel dosimeter using the iris collimator; eight shots using the 5 mm and the 7.5 mm collimators, five using the 10 mm and four using the 12.5 mm and the 15 mm collimators. The robotic mechanism of the couch was used to deliver each radiation shot at predefined locations within the gel dosimeters. The coordinates of these points were chosen based on the off axis profiles of the measured fields and a 0.5% limit for cross talk between adjacent fields. The iris collimator was instructed to fully open before the formation of each field used for radiation shot delivery. One 60 mm msr field shot was also delivered close to the edge of each gel dosimeter for OF calculation [see Eq. (1)] as well as dose-response calibration purposes.[8]

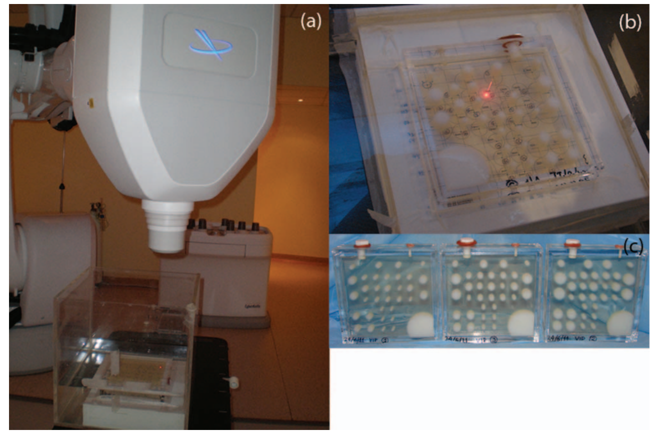

FIG. 1. Photographs depicting [(a), (b)] the experimental setup for the polymer gel dosimetry and (c) the three irradiated gel phantoms (left to right: 650 mm SDD, 800 mm SDD, and 1000 mm SDD).

A nominal dose of 30 Gy at 15 mm depth (taking into account the 8 mm gel container wall thickness) was delivered at the center of each field size. Besides lying within the linear region of the typical dose response calibration curve for the VIP gel,[8,34,35] this dose level results to less than 0.2 Gy dose cross talk between adjacent shots which is well below the VIP gel dose response threshold.[8,34,35] The absence of significant cross talk between adjacent shots is evident in Fig. 1(c).

The polymer gel dosimeters were read out two days post irradiation using a 1.5 Tesla Philips Achieva MRI scanner (Philips Medical Systems, Netherland BV). A volume selective (3D), Carr-Purcell-Meiboom-Gill (CPMG), 32-echo pulse sequence (with an initial echo time (TE) of 40 ms, an interecho time of 40 ms, and a repetition time (TR) of 1800 ms) was used for imaging each gel dosimeter in a separate session. A rectangular 200 × 200 mm^2 field of view and a 400 × 400 image acquisition/reconstruction matrix were employed resulting in an in-plane acquisition resolution of 0.5 × 0.5 mm^2. Twenty-five axial (xy plane) partitions of 0.5 mm thickness were reconstructed for each echo resulting in a voxel size of 0.5 × 0.5 × 0.5 mm^3, since interpolation was not implemented. This voxel size is a compromise between the contradicting demands for submillimeter spatial resolution and acceptable statistical noise.

A single image of NMR spin–spin relaxation time, T_2, was calculated for each slice by fitting a simple log–linear function on the acquired 32-echo train on a pixel by pixel basis, after discarding the first echo due to imperfections in the signal decay curve.[36] The twenty-five T_2 maps obtained were combined to construct a three dimensional relaxation rate, R_2 ($= 1/T_2$) matrix for each gel dosimeter. The plane corresponding to 15 mm depth (taking into account the 8 mm gel container thickness) was defined in the matrix and the center coordinates of each radiation field were calculated using the field symmetry.[8]

The polymer gel dosimeters were calibrated using the off axis data of the 60 mm msr field delivered in each gel dosimeter following a procedure described elsewhere.[8] A linear function of the form of $R_2 = a*D + b$ was fitted to calibration data ranging from 3 Gy to 30 Gy to obtain the sensitivity, a, and the constant term, b, of the dose-response curve of each gel dosimeter, using error weighted least squares fitting routines.

Polymer gel OFs were calculated using the following equation:

$$\mathrm{OF} = \frac{(R_2^{f_{\mathrm{clin}}}(r=0\ \mathrm{mm,\ SDD}) - \mathrm{b})/\mathrm{MU}^{f_{\mathrm{clin}}}}{(R_2^{f_{\mathrm{msr}}}(r=0\ \mathrm{mm,\ SDD}=800\ \mathrm{mm}) - \mathrm{b})/\mathrm{MU}^{f_{\mathrm{msr}}}} \times \left(\frac{\mathrm{SDD}}{800}\right)^2, \quad (3)$$

which was obtained by solving the calibration function for dose and substituting into Eq. (1). The constant term b from the calibration curve of each gel vial was applied to OF measurements in the same vial to preclude uncertainty due to intra batch response variation.

Single voxel polymer gel OF measurements have been shown to suffer from increased uncertainty[8] and therefore the use of a fitting procedure on the average off axis profile data has been suggested.[7,8] This technique was followed for the 5 mm, 7.5 mm, and 10 mm collimators, by fitting a 5th order polynomial function to the corresponding R_2 off axis profiles and calculating the $R_2(r = 0$ mm, SDD) from the fitted function. For the 12.5 mm, 15 mm, and 60 mm collimators, polynomial functions could not describe the measured R_2 off axis profiles. Therefore, a 3 × 3 Wiener low pass filter was applied to the measured R_2 values and the $R_2(r = 0$ mm, SDD) were calculated as the average of voxels lying inside a circle of 2 mm, 3 mm, and 5 mm diameter for the 12.5 mm, 15 mm, and 60 mm collimators, respectively. The obtained $R_2(r = 0$ mm, SDD) results for the same field were averaged and used for the calculation of the corresponding OF.

Volume averaging correction factors were also calculated for the measured small fields using the polymer gel dose distributions. The correction factor was given by the ratio of dose at the center of the field and 15 mm depth, to the average dose within a cylinder centered on this point with 2.5 mm height and varying diameter.[8]

The uncertainty associated with polymer gel OF measurements was estimated using error propagation[30] on (a) the standard deviation of the mean of the $R_2(r = 0$ mm, SDD) values (type A) and (b) the type B uncertainty components associated with the constant term of the calibration curve, the establishment of the desired SSD, and the determination of the plane corresponding to 15 mm depth inside the 3D R_2 matrix ($u_{\mathrm{depth}} = 0.3$ mm calculated assuming rectangular distribution and an uncertainty of ± 1 slice in finding the central axial slice). The type B uncertainty of the radiation field center coordinates was found similar to the corresponding uncertainty in EBT film measurements and therefore excluded from consideration.

III. RESULTS

The uncorrected OFs of the small iris fields measured using the microchamber, the diode detectors, the alanine and TLD pellets, the EBT films, and the polymer gels are presented in Table I and Figs. 2–4 for the 650 mm, 800 mm, and 1000 mm SDD, respectively. A general inspection of the presented data shows large differences between OF results measured with different dosimeters, which decrease with increasing field size and SDD in accordance with corresponding findings in the literature.[1,4,7–10,12] For the 650 mm SDD, maximum differences between OF results measured using different dosimeters are 69%, 25%, 12%, 7%, and 6% for the 5 mm, 7.5 mm, 10 mm, 12.5 mm, and 15 mm collimators, respectively. These maximum differences decrease to 36%, 15%, 7%, 4%, and 2% for the 800 mm SDD, and 25%, 11%, 5%, 3%, and 2% for the 1000 mm SDD. The magnitude of these maximum differences however is partly attributed to the alanine OF results, which are significantly lower than the corresponding OFs measured with the rest of the dosimeters used in this work. This is attributed to the large diameter (5 mm) of

TABLE I. Measured output factors for the 5 mm, 7.5 mm, 10 mm, 12.5 mm, and 15 mm iris collimators for the 650 mm, 800 mm, and 1000 mm SDD values. Corresponding uncertainties at the 68% level are shown in parentheses.

		Detector type								
SDD (mm)	Collimator (mm)	PinPoint 31014	Diode 60017	Diode 60012	Diode 60008	EDGE	TLD	Alanine	EBT films	VIP gels
650	5.0	0.428 (22)	0.534 (6)	0.542 (6)	0.542 (6)	0.539 (6)	0.525 (5)	0.321 (6)	0.505 (12)	0.507 (12)
	7.5	0.707 (16)	0.789 (7)	0.794 (7)	0.798 (7)	0.800 (7)	0.770 (8)	0.641 (11)	0.760 (20)	0.764 (19)
	10.0	0.814 (10)	0.864 (7)	0.869 (7)	0.875 (7)	0.877 (7)	0.845 (15)	0.785 (13)	0.844 (19)	0.851 (15)
	12.5	0.871 (8)	0.904 (7)	0.911 (8)	0.912 (8)	0.917 (8)	0.886 (12)	0.853 (13)	0.876 (18)	0.914 (15)
	15.0	0.907 (8)	0.930 (8)	0.937 (8)	0.935 (8)	0.941 (8)	0.925 (11)	0.892 (14)	0.917 (19)	0.938 (18)
800	5.0	0.452 (19)	0.523 (5)	0.534 (5)	0.544 (6)	0.528 (5)	0.513 (5)	0.400 (8)	0.496 (10)	0.514 (14)
	7.5	0.745 (13)	0.802 (6)	0.808 (6)	0.823 (6)	0.817 (6)	0.786 (9)	0.717 (11)	0.782 (16)	0.788 (19)
	10.0	0.854 (8)	0.884 (6)	0.887 (7)	0.900 (7)	0.898 (6)	0.848 (10)	0.844 (13)	0.872 (19)	0.847 (16)
	12.5	0.904 (7)	0.920 (7)	0.923 (6)	0.931 (7)	0.933 (7)	0.912 (9)	0.897 (14)	0.910 (19)	0.916 (16)
	15.0	0.934 (7)	0.941 (7)	0.943 (6)	0.949 (7)	0.951 (7)	0.935 (10)	0.930 (15)	0.940 (21)	0.944 (17)
1000	5.0	0.467 (14)	0.511 (4)	0.523 (5)	0.527 (5)	0.516 (4)	0.503 (5)	0.421 (7)	0.490 (11)	0.513 (16)
	7.5	0.775 (13)	0.806 (6)	0.810 (6)	0.819 (5)	0.818 (5)	0.795 (10)	0.739 (12)	0.804 (18)	0.778 (17)
	10.0	0.888 (9)	0.900 (6)	0.900 (6)	0.912 (6)	0.911 (6)	0.881 (9)	0.871 (17)	0.894 (19)	0.877 (26)
	12.5	0.930 (7)	0.931 (6)	0.931 (7)	0.939 (6)	0.939 (6)	0.928 (8)	0.916 (14)	0.932 (20)	0.933 (25)
	15.0	0.952 (7)	0.948 (6)	0.947 (7)	0.952 (6)	0.953 (6)	0.940 (9)	0.936 (14)	0.953 (21)	0.948 (25)

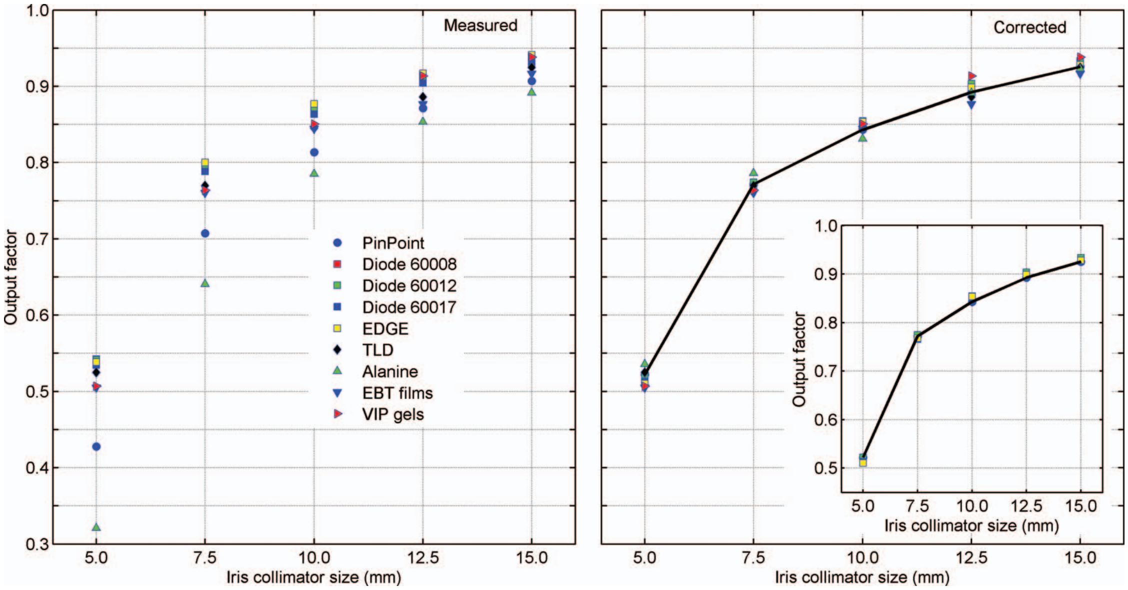

FIG. 2. Measured (left) and corrected (right) output factors for 650 mm SDD, plotted as a function of iris collimator size. Diode measurements were corrected using the MC derived $k^{f_{\mathrm{clin}},f_{\mathrm{msr}}}_{Q_{\mathrm{clin}},Q_{\mathrm{msr}}}$ correction factors for the 800 mm SDD given in Ref. 37, while PinPoint measurements were corrected using the corresponding, experimentally derived $k^{f_{\mathrm{clin}},f_{\mathrm{msr}}}_{Q_{\mathrm{clin}},Q_{\mathrm{msr}}}$ of this work. The alanine, TLD, EBT, and gel error weighted average output factor values are shown with a solid line. The insert figure on the right shows a more detailed comparison of the corrected output factors obtained using the most commonly used detectors (i.e., diodes and microchambers only) with the alanine, TLD, EBT, and gel weighted average.

the alanine detectors, which introduced significant volume averaging effects (see Sec. II.B) especially for the smaller fields (please note that the 5 mm collimator corresponds to actual field sizes of 4.1 mm and 6.3 mm at 650 mm and 1000 mm SDD, respectively). If alanine OF results are excluded, the above-mentioned maximum differences decrease to 27%, 20%, and 13% for the smallest 5 mm collimator at 650 mm, 800 mm, and 1000 mm SDD, respectively.

Despite the substantial underestimation observed in the alanine results, these detectors have been found capable of providing accurate OF results for small fields when corrected for volume averaging.[14] Volume averaging correction factor results are presented in Fig. 5 as a function of detector diameter for the measured collimator sizes at 650 mm, 800 mm, and 1000 mm SDDs. Based on these data the volume averaging correction factors for the alanine measurements were calculated and results are presented

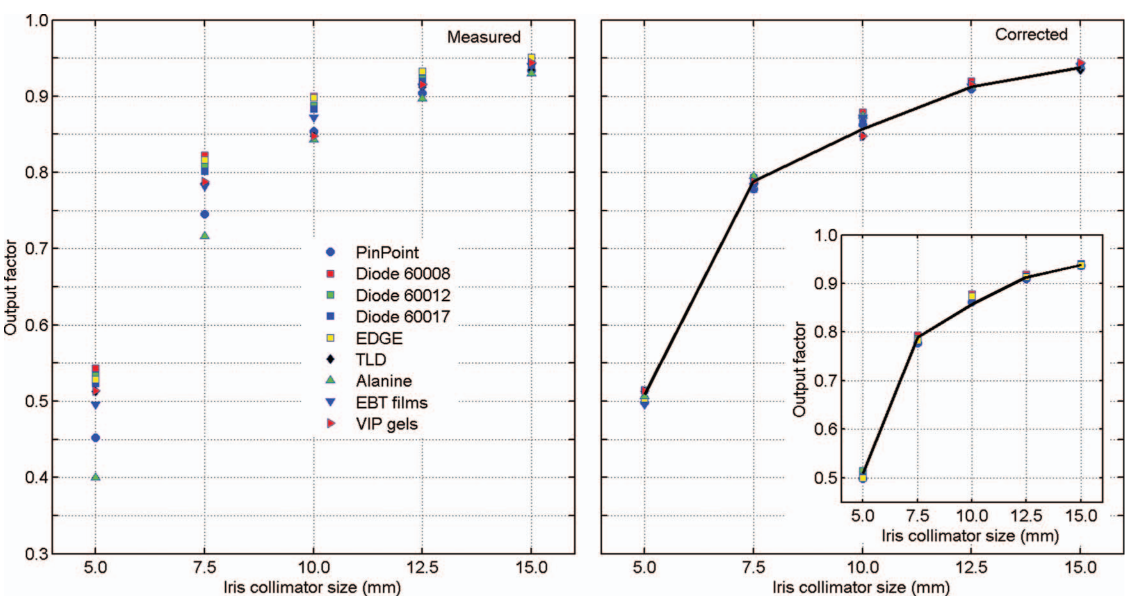

FIG. 3. Measured (left) and corrected (right) output factors for 800 mm SDD, plotted as a function of iris collimator size. Diode and PinPoint measurements were corrected using the MC derived $k^{f_{\mathrm{clin}},f_{\mathrm{msr}}}_{Q_{\mathrm{clin}},Q_{\mathrm{msr}}}$ correction factors given in Ref. 37. The alanine, TLD, EBT, and gel error weighted average output factor values are shown with a solid line. The insert figure on the right shows a more detailed comparison of the corrected output factors obtained using the most commonly used detectors (i.e., diodes and microchambers only) with the alanine, TLD, EBT, and gel weighted average.

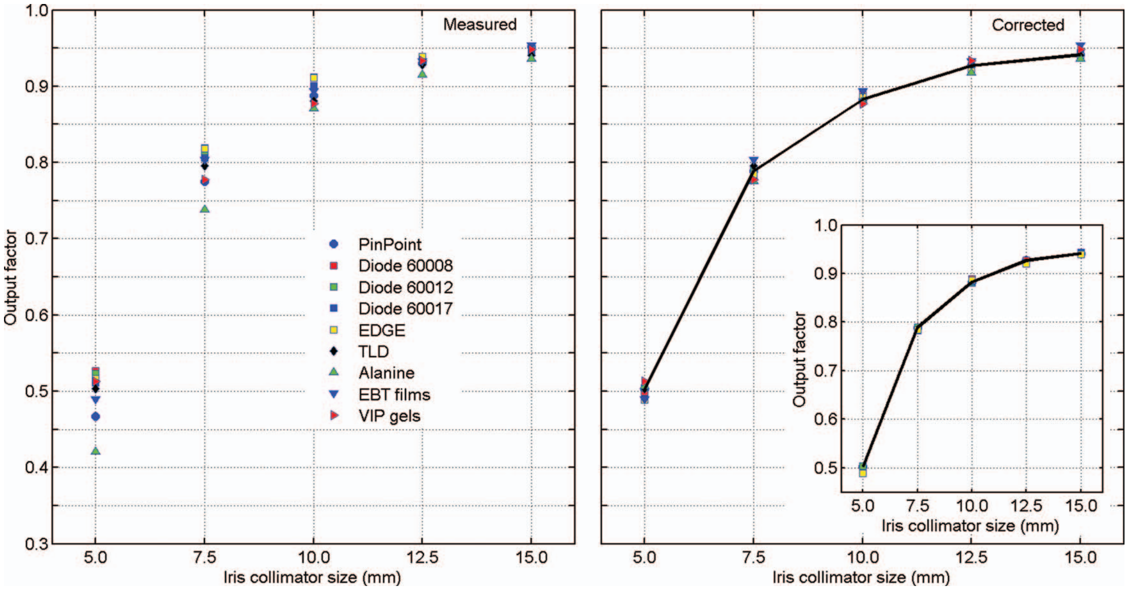

FIG. 4. Measured (left) and corrected (right) output factors for 1000 mm SDD, plotted as a function of iris collimator size. Diode measurements were corrected using the MC derived $k^{f_{\mathrm{clin}},f_{\mathrm{msr}}}_{Q_{\mathrm{clin}},Q_{\mathrm{msr}}}$ correction factors for the 800 mm SDD given in Ref. 37, while PinPoint measurements were corrected using the corresponding, experimentally derived $k^{f_{\mathrm{clin}},f_{\mathrm{msr}}}_{Q_{\mathrm{clin}},Q_{\mathrm{msr}}}$ of this work. The alanine, TLD, EBT, and gel error weighted average output factor values are shown with a solid line. The insert figure on the right shows a more detailed comparison of the corrected output factors obtained using the most commonly used detectors (i.e., diodes and microchambers only) with the alanine, TLD, EBT, and gel weighted average.

in Table II for the iris collimators and SDDs used in this study.

Comparison of the OF results measured at the reference SDD of 800 mm using the polymer gels, EBT films, alanine (corrected for volume averaging), and TLD dosimeters shows a good agreement with corresponding error weighted average values (within 2.7%, 1%, 2%, 0.3%, and 0.6%, for the 5 mm, 7.5 mm, 10 mm, 12.5 mm, and 15 mm collimators, respectively). A similar comparison of the OF results measured at 650 mm and 1000 mm SDD shows differences of less than 3.3%, 1.8%, 1.4%, 2.4%, 1.4% and 2.6%, 1.9%, 1.3%, 0.9%,

TABLE II. Alanine volume averaging correction factors for the 5 mm, 7.5 mm, 10 mm, 12.5 mm, and 15 mm iris collimators, and the 650 mm, 800 mm, and 1000 mm SDD values. Corresponding uncertainties at the 68% level are shown in parentheses.

	Collimator				
SDD (mm)	5.0 mm	7.5 mm	10.0 mm	12.5 mm	15.0 mm
650	1.668 (8)	1.226 (7)	1.059 (10)	1.045 (5)	1.035 (4)
800	1.268 (11)	1.110 (4)	1.037 (5)	1.016 (5)	1.010 (1)
1000	1.204 (3)	1.050 (3)	1.011 (3)	1.003 (3)	1.000 (1)

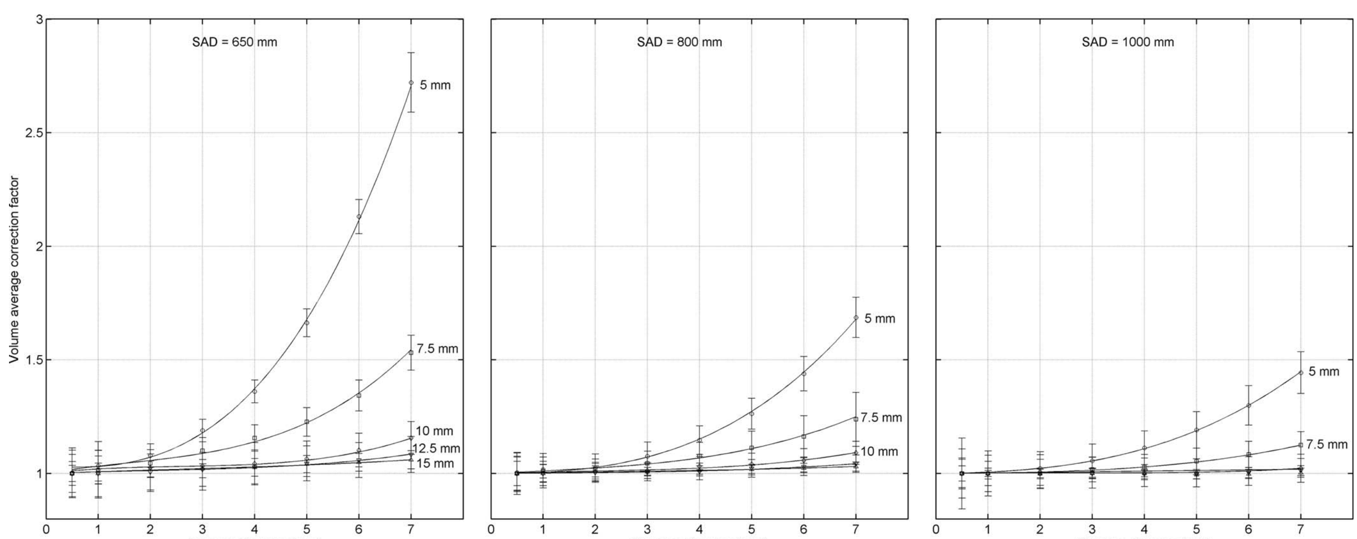

FIG. 5. Volume averaging correction factors for the 5 mm, 7.5 mm, 10 mm, 12.5 mm, and 15 mm iris collimators plotted as a function of detector diameter for (a) 650 mm, (b) 800 mm, and (c) 1000 mm SDD.

TABLE III. Microchamber and diode detector $k_{Q_{\rm clin},Q_{\rm msr}}^{f_{\rm clin},f_{\rm msr}}$ correction factors for the 5 mm, 7.5 mm, 10 mm, 12.5 mm, and 15 mm iris collimators, for the 650 mm, 800 mm, and 1000 mm SDD values. Corresponding uncertainties at the 68% level are shown in parentheses.

Detector	Collimator 5.0 mm	7.5 mm	10.0 mm	12.5 mm	15.0 mm
	SDD = 650 mm				
PinPoint 31014	1.220 (28)	1.091 (18)	1.036 (13)	1.024 (11)	1.020 (11)
Diode 60017	0.977 (7)	0.979 (9)	0.976 (11)	0.987 (10)	0.995 (11)
Diode 60012	0.964 (7)	0.972 (9)	0.970 (10)	0.980 (10)	0.987 (11)
Diode 60008	0.963 (7)	0.967 (9)	0.963 (10)	0.978 (10)	0.990 (11)
EDGE	0.969 (7)	0.965 (9)	0.961 (10)	0.973 (10)	0.983 (11)
	SDD = 800 mm				
PinPoint 31014	1.127 (22)	1.058 (15)	1.003 (10)	1.009 (10)	1.004 (10)
Diode 60017	0.973 (6)	0.983 (8)	0.969 (9)	0.992 (9)	0.997 (10)
Diode 60012	0.954 (6)	0.976 (8)	0.965 (9)	0.989 (8)	0.994 (9)
Diode 60008	0.937 (7)	0.958 (8)	0.952 (9)	0.980 (9)	0.988 (10)
EDGE	0.964 (6)	0.965 (8)	0.954 (9)	0.978 (9)	0.986 (10)
	SDD = 1000 mm				
PinPoint 31014	1.077 (16)	1.018 (15)	0.994 (12)	0.997 (10)	0.989 (10)
Diode 60017	0.985 (6)	0.978 (8)	0.980 (9)	0.995 (9)	0.993 (9)
Diode 60012	0.961 (6)	0.973 (9)	0.980 (9)	0.995 (9)	0.994 (10)
Diode 60008	0.954 (6)	0.963 (8)	0.968 (9)	0.987 (9)	0.988 (9)
EDGE	0.974 (6)	0.964 (8)	0.969 (9)	0.987 (9)	0.988 (9)

1.3%, respectively. In view of the excellent agreement between the polymer gel, EBT, alanine, and TLD measured OFs, the corresponding error weighted average values were used to calculate the $k_{Q_{\rm clin},Q_{\rm msr}}^{f_{\rm clin},f_{\rm msr}}$ correction factors of the microchamber and diode detectors used in this work. The uncertainty of the obtained $k_{Q_{\rm clin},Q_{\rm msr}}^{f_{\rm clin},f_{\rm msr}}$ correction factors was calculated using error propagation on the uncertainty of the measured OFs using the microchamber and diodes and the uncertainty of the error weighted average OF values.

The calculated $k_{Q_{\rm clin},Q_{\rm msr}}^{f_{\rm clin},f_{\rm msr}}$ correction factors are presented in Table III for the microchamber, the PTW-60017, −60012, −60008 diodes, and the EDGE detector for the 5 mm, 7.5 mm, 10 mm, 12.5 mm, and 15 mm collimators and the 650 mm, 800 mm, and 1000 mm SDDs. A general inspection of the presented data reveals that the $k_{Q_{\rm clin},Q_{\rm msr}}^{f_{\rm clin},f_{\rm msr}}$ for the microchamber is greater than unity with values ranging between 1.127 ± 0.022 (for the 5 mm collimator) and 1.004 ± 0.010 (for the 15 mm collimator) at the reference SDD of 800 mm. Furthermore, the $k_{Q_{\rm clin},Q_{\rm msr}}^{f_{\rm clin},f_{\rm msr}}$ of the PinPoint depends on the SDD taking values of 1.220 ± 0.028 and 1.077 ± 0.016 for the 5 mm collimator at 650 mm and 1000 mm SDD, respectively. On the contrary, the $k_{Q_{\rm clin},Q_{\rm msr}}^{f_{\rm clin},f_{\rm msr}}$ correction factor for the diode detectors are all lower than unity and equal to 0.973 ± 0.006, 0.954 ± 0.006, 0.937 ± 0.007, and 0.964 ± 0.006 for the PTW-60017, −60012, −60008 diodes, and the EDGE detector, respectively, for the 5 mm collimator and the reference 800 mm SDD. Comparison of the corresponding $k_{Q_{\rm clin},Q_{\rm msr}}^{f_{\rm clin},f_{\rm msr}}$ correction factors for the same collimator at 650 mm, 800 mm, and 1000 mm SDD shows agreement within uncertainties, suggesting that $k_{Q_{\rm clin},Q_{\rm msr}}^{f_{\rm clin},f_{\rm msr}}$ for the diodes does not depend on SDD.

IV. DISCUSSION

OF results in Table I measured for the 800 mm reference SDD using different detectors show large differences (36% for the 5 mm collimator decreasing to 2% for the 15 mm collimator). These findings are similar to corresponding differences of 33% and 2.6% found in a previous work reporting on OF measurements of CK small fields defined using fixed collimators.[14] These differences are increased for the 650 mm SDD reaching up to 69% (for the 5 mm collimator) and 7% (for the 15 mm collimator), and decreased to 25% (for the 5 mm collimator) and 2% (for the 15 mm collimator) for the 1000 mm SDD. The observed differences are attributed to the dosimetric characteristics of the dosimeters used in this work. In specific, diode detectors have been reported to overestimate small field OFs,[8,9,12,14,17] an effect that has been attributed to the perturbation of the local particle fluence caused by the presence of the small but relatively dense ($\rho = 2.33$ g cm^{-3}) silicon detector in the field.[17] Small cavity ion chambers, on the other hand, underestimate small field OFs due to volume averaging effects combined with the difference in the fluence perturbation caused by the presence of the chamber in the small fields and the msr field.[14] Volume averaging in the relatively large diameter (5 mm) of the sensitive volume of the alanine dosimeters explains the largest OF underestimation observed in measurements for the smallest fields.

Experimentally derived $k_{Q_{\rm clin},Q_{\rm msr}}^{f_{\rm clin},f_{\rm msr}}$ correction factors for the PinPoint and the diode detectors used in this work are given in Table III. $k_{Q_{\rm clin},Q_{\rm msr}}^{f_{\rm clin},f_{\rm msr}}$ values results of this work for the PinPoint, the unshielded PTW-60017 and the shielded PTW-60008 diodes are plotted as a function of iris collimator size for the 800 mm reference SDD in Fig. 6 along with correction factor corresponding results calculated independently

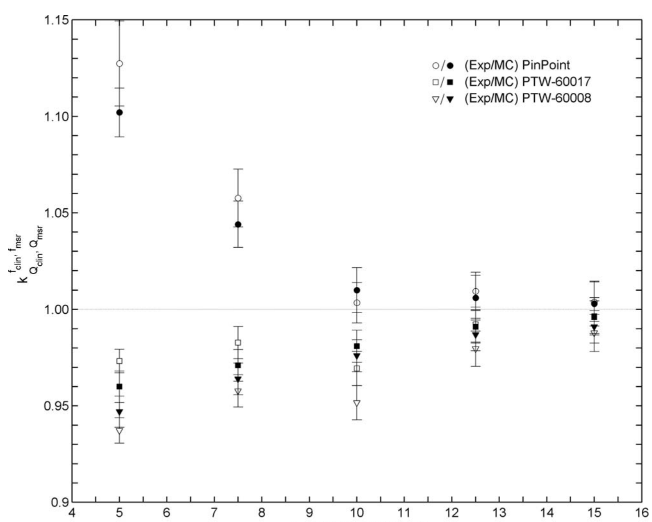

FIG. 6. Measured $k_{Q_{\rm clin},Q_{\rm msr}}^{f_{\rm clin},f_{\rm msr}}$ correction factors for 800 mm SDD plotted as a function of iris collimator size for the PinPoint 31014 microchamber, PTW-60017 unshielded, and PTW-60008 shielded diodes. Corresponding results calculated using MC simulation by Francescon *et al.* (Ref. 37) are plotted for comparison. The uncertainty, at 68% confidence level, of the presented correction factor results are depicted using error bars.

using MC simulation.[37] A close agreement can be observed between experimental and MC calculated $k_{Q_{\mathrm{clin}},Q_{\mathrm{msr}}}^{f_{\mathrm{clin}},f_{\mathrm{msr}}}$ correction factors for most collimators (within 2%, 1%, 0.7%, and 0.3% for the 5 mm, 7.5 mm, 12.5 mm, and 15 mm collimators, respectively). The largest difference is for the 10 mm collimator where differences are up to 2.5% and the measured factors are lower than the MC calculated values for all three detectors. For the 10 mm collimator, the $k_{Q_{\mathrm{clin}},Q_{\mathrm{msr}}}^{f_{\mathrm{clin}},f_{\mathrm{msr}}}$ correction factors measured for the diode also deviate from the expected trend of increasing $k_{Q_{\mathrm{clin}},Q_{\mathrm{msr}}}^{f_{\mathrm{clin}},f_{\mathrm{msr}}}$ with collimator size observed at other collimator sizes. Nevertheless, the 2.5% difference lies within the range of experimental and MC uncertainties and therefore the two datasets are consistent at all collimator sizes.

Regarding the microchamber, results presented in Table III show that overall $k_{Q_{\mathrm{clin}},Q_{\mathrm{msr}}}^{f_{\mathrm{clin}},f_{\mathrm{msr}}}$ decreases with increasing collimator size and SDD. This is attributed to changes in the lateral electron fluence disequilibrium and volume averaging effects. Moreover, based on the volume averaging correction factor data presented in Fig. 5 and given the PinPoint air cavity diameter (Ø 2 mm), the contribution of volume averaging effect to $k_{Q_{\mathrm{clin}},Q_{\mathrm{msr}}}^{f_{\mathrm{clin}},f_{\mathrm{msr}}}$ is of the order of 7%, 3%, and 2% for the smallest 5 mm collimator at 650 mm, 800 mm, and 1000 mm SDD, respectively. Comparison of these findings with the corresponding $k_{Q_{\mathrm{clin}},Q_{\mathrm{msr}}}^{f_{\mathrm{clin}},f_{\mathrm{msr}}}$ results of 1.220, 1.127, and 1.077 for the 5 mm collimator suggests that the effect of the different fluence perturbations caused by the presence of the chamber in the small fields compared to the msr field is up to 15%, 10%, and 6% at 650 mm, 800 mm, and 1000 mm SDD, respectively. It should be noted that the magnitude of the volume averaging effect depends on chamber orientation and it is expected to increase substantially if the chamber was positioned with its stem perpendicular to the beam axis, increasing the $k_{Q_{\mathrm{clin}},Q_{\mathrm{msr}}}^{f_{\mathrm{clin}},f_{\mathrm{msr}}}$ correction factors for the microchamber correspondingly. Finally, the observed dependence of $k_{Q_{\mathrm{clin}},Q_{\mathrm{msr}}}^{f_{\mathrm{clin}},f_{\mathrm{msr}}}$ with SDD for the microchamber suggests that the MC derived $k_{Q_{\mathrm{clin}},Q_{\mathrm{msr}}}^{f_{\mathrm{clin}},f_{\mathrm{msr}}}$ values for 800 mm SDD should not be applied for 650 mm and 1000 mm SDDs with this detector.

Diode detector results in Table III show an increase of $k_{Q_{\mathrm{clin}},Q_{\mathrm{msr}}}^{f_{\mathrm{clin}},f_{\mathrm{msr}}}$ correction factors for the 800 mm SDD with collimator size with the unshielded PTW-60017 requiring smaller corrections (i.e., $k_{Q_{\mathrm{clin}},Q_{\mathrm{msr}}}^{f_{\mathrm{clin}},f_{\mathrm{msr}}}$ closer to unity) compared to the shielded PTW-60008 and the EDGE detector. The larger corrections required for the shielded diodes is attributed to the increased perturbation of the local particle fluence caused by the presence of tungsten or copper high atomic number materials used as backing mediums in the PTW-60008 and the EDGE detector, respectively.[17] Diode $k_{Q_{\mathrm{clin}},Q_{\mathrm{msr}}}^{f_{\mathrm{clin}},f_{\mathrm{msr}}}$ correction factors for the 650 mm and 1000 mm SDD were found to agree with corresponding results at 800 mm SDD within 1.2%, 1.5%, 2.7%, and 1.6%, for the PTW-60017, −60012, −60008, and the EDGE diode detectors, respectively. In view of the experimental uncertainties ascribed to these $k_{Q_{\mathrm{clin}},Q_{\mathrm{msr}}}^{f_{\mathrm{clin}},f_{\mathrm{msr}}}$ results, this finding suggests that the correction factors of the diode detectors do not depend on SDD.

The OFs measured using the PinPoint and the diode detectors were corrected according to the dosimetric formalism suggested for small and nonstandard fields.[18] In view of the independence of $k_{Q_{\mathrm{clin}},Q_{\mathrm{msr}}}^{f_{\mathrm{clin}},f_{\mathrm{msr}}}$ on SDD observed in this work, the MC calculated $k_{Q_{\mathrm{clin}},Q_{\mathrm{msr}}}^{f_{\mathrm{clin}},f_{\mathrm{msr}}}$ correction factor values at 800 mm SDD[37] were used to correct the diode measured OFs for the 650 mm, 800 mm, and 1000 mm SDD. For the PinPoint microchamber on the other hand, the MC calculated $k_{Q_{\mathrm{clin}},Q_{\mathrm{msr}}}^{f_{\mathrm{clin}},f_{\mathrm{msr}}}$ correction factor values were applied only to the OF results measured for the 800 mm SDD (MC calculated $k_{Q_{\mathrm{clin}},Q_{\mathrm{msr}}}^{f_{\mathrm{clin}},f_{\mathrm{msr}}}$ values were available only at this SDD), while for the 650 mm and 1000 mm SDDs the measured OFs were corrected using the corresponding experimentally derived $k_{Q_{\mathrm{clin}},Q_{\mathrm{msr}}}^{f_{\mathrm{clin}},f_{\mathrm{msr}}}$ values presented in Table III.

The corrected OFs, $\Omega_{Q_{\mathrm{clin}},Q_{\mathrm{msr}}}^{f_{\mathrm{clin}},f_{\mathrm{msr}}}$, are summarized in Table IV and presented graphically in Figs. 2–4 as a function of collimator size for the 650 mm, 800 mm, and 1000 mm SDDs, respectively. In the same figures the corresponding polymer gel, EBT, alanine, and TLD OF results as well as the corresponding error weighted average OF values are also included for comparison.

A general inspection of the $\Omega_{Q_{\mathrm{clin}},Q_{\mathrm{msr}}}^{f_{\mathrm{clin}},f_{\mathrm{msr}}}$ results in Figs. 2–4 shows that the large differences observed between the measured (uncorrected) OFs are reduced to less than 6.1%, 3.8%, and 2.6% for the 650 mm, 800 mm, and 1000 mm SDD. PinPoint and diode detector $\Omega_{Q_{\mathrm{clin}},Q_{\mathrm{msr}}}^{f_{\mathrm{clin}},f_{\mathrm{msr}}}$ results for the 800 mm reference SDD (calculated using MC derived $k_{Q_{\mathrm{clin}},Q_{\mathrm{msr}}}^{f_{\mathrm{clin}},f_{\mathrm{msr}}}$ correction factors from the literature) were found to agree within 2.2%, 1.3%, 2.6%, 0.7%, and 0.2% with the corresponding alanine, TLD, EBT, and polymer gel error weighted average OFs (Table IV), for the 5 mm, 7.5 mm, 10 mm, 12.5 mm, and 15 mm collimators, respectively. The largest difference of 2.6% was observed for the PTW-60008 diode (see also the inset of Fig. 3). Similarly, a close agreement is observed between the PinPoint and diode $\Omega_{Q_{\mathrm{clin}},Q_{\mathrm{msr}}}^{f_{\mathrm{clin}},f_{\mathrm{msr}}}$ with the corresponding alanine, TLD, EBT, and polymer gel error weighted average OFs for the 650 mm and 1000 mm SDD. This agreement is within 2.3%, 0.8%, 1.3%, 1.2%, and 0.9% for the 650 mm SDD (see inset of Fig. 2) and 2.8%, 0.8%, 0.9%, 0.8%, and 0.2% for the 1000 mm SDD (see inset of Fig. 4), for the 5 mm, 7.5 mm, 10 mm, 12.5 mm, and 15 mm collimators, respectively.

The error weighted $\Omega_{Q_{\mathrm{clin}},Q_{\mathrm{msr}}}^{f_{\mathrm{clin}},f_{\mathrm{msr}}}$ results for the 650 mm SDD were found equal to 0.518 ± 0.003, 0.770 ± 0.004, 0.849 ± 0.004, 0.897 ± 0.004, and 0.927 ± 0.004, for the 5 mm, 7.5 mm, 10 mm, 12.5 mm, and 15 mm iris collimators, respectively. For the 800 mm and the 1000 mm SDD, error weighted $\Omega_{Q_{\mathrm{clin}},Q_{\mathrm{msr}}}^{f_{\mathrm{clin}},f_{\mathrm{msr}}}$ results were 0.508 ± 0.002, 0.786 ± 0.003, 0.866 ± 0.004, 0.914 ± 0.004, and 0.938 ± 0.004, and of 0.498 ± 0.002, 0.787 ± 0.004, 0.884 ± 0.004, 0.925 ± 0.004, and 0.942 ± 0.004, respectively. The error weighted average values form a consensus $\Omega_{Q_{\mathrm{clin}},Q_{\mathrm{msr}}}^{f_{\mathrm{clin}},f_{\mathrm{msr}}}$ data set for the small fields of the iris collimator on this specific CK system.

Consensus $\Omega_{Q_{\mathrm{clin}},Q_{\mathrm{msr}}}^{f_{\mathrm{clin}},f_{\mathrm{msr}}}$ values increase with increasing SDD for all but the smallest, 5 mm collimator where an inverse trend can be observed. This can be attributed to the combined effect of phantom scatter and source occlusion variation with SDD. Specifically, phantom scatter, and consequently $\Omega_{Q_{\mathrm{clin}},Q_{\mathrm{msr}}}^{f_{\mathrm{clin}},f_{\mathrm{msr}}}$, increases with SDD, but so does the proportion of

TABLE IV. Corrected output factors, $\Omega_{Q_{clin},Q_{msr}}^{f_{clin},f_{msr}}$, for the 5 mm, 7.5 mm, 10 mm, 12.5 mm, and 15 mm iris collimators for the 650 mm, 800 mm, and 1000 mm SDD values. Diode measurements were corrected using the corresponding MC derived $k_{Q_{clin},Q_{msr}}^{f_{clin},f_{msr}}$ correction factors of Francescon *et al.* (Ref. 37) PinPoint measurements at 800 mm SDD were corrected using the MC derived $k_{Q_{clin},Q_{msr}}^{f_{clin},f_{msr}}$ correction factors, while at 650 mm and 1000 mm SDD were corrected using the experimentally derived $k_{Q_{clin},Q_{msr}}^{f_{clin},f_{msr}}$ correction factors of Table III. Corresponding uncertainties at the 68% level are shown in parentheses.

		Detector type					
SDD (mm)	Collimator (mm)	PinPoint 31014	Diode 60017	Diode 60012	Diode 60008	EDGE	Alanine, TLD, EBT, gel error weighted average
650	5.0	0.522 (30)	0.513 (7)	0.522 (7)	0.514 (7)	0.510 (7)	0.522 (4)
	7.5	0.772 (21)	0.766 (9)	0.774 (9)	0.769 (9)	0.767 (9)	0.772 (8)
	10.0	0.843 (14)	0.847 (10)	0.851 (10)	0.854 (10)	0.853 (10)	0.843 (8)
	12.5	0.892 (13)	0.896 (11)	0.903 (11)	0.900 (11)	0.899 (11)	0.892 (7)
	15.0	0.925 (13)	0.927 (11)	0.933 (11)	0.926 (11)	0.926 (11)	0.925 (7)
800	5.0	0.498 (22)	0.502 (6)	0.515 (6)	0.515 (7)	0.506 (6)	0.509 (4)
	7.5	0.778 (16)	0.779 (9)	0.787 (8)	0.793 (9)	0.783 (9)	0.788 (6)
	10.0	0.862 (13)	0.867 (10)	0.869 (10)	0.879 (10)	0.874 (10)	0.857 (7)
	12.5	0.909 (10)	0.911 (10)	0.916 (10)	0.919 (10)	0.914 (10)	0.913 (6)
	15.0	0.937 (13)	0.937 (10)	0.940 (10)	0.941 (11)	0.938 (10)	0.938 (7)
1000	5.0	0.503 (17)	0.490 (6)	0.504 (7)	0.499 (6)	0.489 (6)	0.503 (4)
	7.5	0.789 (17)	0.783 (9)	0.790 (9)	0.789 (9)	0.785 (8)	0.789 (7)
	10.0	0.882 (14)	0.883 (9)	0.881 (10)	0.890 (9)	0.886 (9)	0.882 (7)
	12.5	0.927 (11)	0.923 (10)	0.924 (10)	0.927 (10)	0.920 (10)	0.927 (7)
	15.0	0.941 (11)	0.944 (10)	0.943 (10)	0.944 (10)	0.939 (10)	0.941 (7)

the source that is obscured from the measuring point, which decreases $\Omega_{Q_{clin},Q_{msr}}^{f_{clin},f_{msr}}$. While, the first effect is present for all collimator sizes (being more important for the smaller ones), the second effect is only relevant to the smallest collimator sizes since once the aperture is large enough for the entire source to be "seen" from the measuring point, this effect disappears. Therefore, the increase of $\Omega_{Q_{clin},Q_{msr}}^{f_{clin},f_{msr}}$ with SDD for all collimators except the 5 mm one where the opposite trend is seen could be explained if beam occlusion dominates for the 5 mm collimator, and phantom scatter dominates for all larger collimator sizes. Corresponding results for the 5 mm fixed collimators show an increase with increasing SDD. The difference in the OF versus SDD trend seen with 5 mm fixed versus 5 mm iris collimators could be explained by the increased length of the iris collimator (∼13 cm versus ∼7 cm for the fixed collimator). Given that the distance to the distal surface of the collimators is the same (400 mm), the top surface of the iris collimator is closer to the source and thus the physical aperture is smaller and the source occlusion greater for the same radiation field size.

V. CONCLUSIONS

Polymer gels, EBT films, alanine pellets, and TLD microcubes were used to measure the $k_{Q_{clin},Q_{msr}}^{f_{clin},f_{msr}}$ correction factors necessary for CyberKnife iris collimator small field OF measurements using one microchamber and four diode detectors at 650 mm, 800 mm, and 1000 mm SDDs. Large interdetector differences of up to 69%, 36%, and 25% were observed between the (uncorrected) measured OFs for the smallest, 5 mm collimator. The experimentally determined $k_{Q_{clin},Q_{msr}}^{f_{clin},f_{msr}}$ correction factors for the PinPoint and diode detectors at 800 mm SDD were found to be in good agreement with corresponding correction factor values determined independently using MC simulation. The experimentally measured $k_{Q_{clin},Q_{msr}}^{f_{clin},f_{msr}}$ correction factor for the PinPoint ranged from 1.127 ± 0.022 (5 mm collimator) to 1.004 ± 0.010 (15 mm collimator) at the reference SDD of 800 mm. A dependence of the $k_{Q_{clin},Q_{msr}}^{f_{clin},f_{msr}}$ correction factor with SDD was also observed for the PinPoint; values were 1.220 ± 0.028 and 1.077 ± 0.016 for the 5 mm collimator and the 650 mm and 1000 mm SDD, respectively. On the contrary, no correlation of the diode $k_{Q_{clin},Q_{msr}}^{f_{clin},f_{msr}}$ correction factors with SDD was observed. The $k_{Q_{clin},Q_{msr}}^{f_{clin},f_{msr}}$ of the diode detectors were equal to 0.973 ± 0.006, 0.954 ± 0.006, 0.937 ± 0.007, and 0.964 ± 0.006 for the PTW-60017, −60012, −60008, and SunNuclear EDGE diode detectors, respectively, for the 5 mm collimator for the 800 mm SDD. The corresponding correction factors for the 15 mm collimator were 0.997 ± 0.010, 0.994 ± 0.009, 0.988 ± 0.010, and 0.986 ± 0.010, respectively. The large differences observed between OF measurements using different detectors were reduced to maximum differences of 6.1%, 3.8%, and 5% for the 650 mm, 800 mm, and 1000 mm SDD when appropriate correction factors were employed, with the largest differences exhibited between alanine and film dosimetry results. Differences between the corrected diode and microchamber measurements relative to the error weighted average of the alanine, TLD, EBT, and polymer gel measurements were ≤2.8% at all collimator sizes and SDDs.

ACKNOWLEDGMENTS

The work was partly supported by Accuray Inc. A. Moutsatsos was exclusively supported by the European Union (European Social Fund – ESF) and Greek national funds through the Operational Program "Education and Lifelong Learning" of the National Strategic Reference Framework (NSRF) -

Research Funding Program: Heracleitus II. Investing in knowledge society through the European Social Fund. The authors would also like to acknowledge the contribution of Dr. Francescon for sharing the MC calculated correction factors for the iris small fields and of Mu Young Lee, Accuray Inc., for lending the PTW 60017 diode and the EDGE detector, as well as for the helpful discussions.

[a)]Author to whom correspondence should be addressed. Electronic mail: vpantelis@phys.uoa.gr

[1]M. M. Aspradakis, J. P. Byrne, H. Palmans, K. Conway, K. Rosser, A. P. Warrington, and S. Duane, "Small field MV photon dosimetry," IPEM Report 103 (IPEM, York, UK, 2010).
[2]I. J. Das, G. X. Ding, and A. Ahnesjo, "Small fields: Nonequilibrium radiation dosimetry," Med. Phys. **35**, 206–215 (2008).
[3]J. Fan, K. Paskalev, L. Wang, L. Jin, J. Li, A. Eldeeb, and C. Ma, "Determination of output factors for stereotactic radiosurgery beams," Med. Phys. **36**, 5292–5300 (2009).
[4]P. Francescon, S. Cora, C. Cavedon, P. Scalchi, S. Reccanello, and F. Colombo, "Use of a new type of radiochromic film, a new parallel-plate micro-chamber, MOSFETs, and TLD 800 microcubes in the dosimetry of small beams," Med. Phys. **25**, 503–511 (1998).
[5]M. Heydarian, P. W. Hoban, and A. H. Beddoe, "A comparison of dosimetry techniques in stereotactic radiosurgery," Phys. Med. Biol. **41**, 93–110 (1996).
[6]W. U. Laub and T. Wong, "The volume effect of detectors in the dosimetry of small fields used in IMRT," Med. Phys. **30**, 341–347 (2003).
[7]A. Moutsatsos, L. Petrokokkinos, P. Karaiskos, P. Papagiannis, E. Georgiou, K. Dardoufas, P. Sandilos, M. Torrens, E. Pantelis, I. Kantemiris, L. Sakelliou, and I. Seimenis, "Gamma Knife output factor measurements using VIP polymer gel dosimetry," Med. Phys. **36**, 4277–4287 (2009).
[8]E. Pantelis, C. Antypas, L. Petrokokkinos, P. Karaiskos, P. Papagiannis, M. Kozicki, E. Georgiou, L. Sakelliou, and I. Seimenis, "Dosimetric characterization of CyberKnife radiosurgical photon beams using polymer gels," Med. Phys. **35**, 2312–2320 (2008).
[9]O. A. Sauer and J. Wilbert, "Measurement of output factors for small photon beams," Med. Phys. **34**, 1983–1988 (2007).
[10]X. R. Zhu, J. J. Allen, J. Shi, and W. E. Simon, "Total scatter factors and tissue maximum ratios for small radiosurgery fields: Comparison of diode detectors, a parallel-plate ion chamber, and radiographic film," Med. Phys. **27**, 472–477 (2000).
[11]M. Westermark, J. Arndt, B. Nilsson, and A. Brahme, "Comparative dosimetry in narrow high-energy photon beams," Phys. Med. Biol. **45**, 685–702 (2000).
[12]P. Francescon, S. Cora, and C. Cavedon, "Total scatter factors of small beams: A multidetector and Monte Carlo study," Med. Phys. **35**, 504–513 (2008).
[13]P. Francescon, S. Cora, C. Cavedon, and P. Scalchi, "Application of a Monte Carlo-based method for total scatter factors of small beams to new solid state micro-detectors," J. Appl. Clin. Med. Phys. **10**, 147–152 (2009).
[14]E. Pantelis, A. Moutsatsos, K. Zourari, W. Kilby, C. Antypas, P. Papagiannis, P. Karaiskos, E. Georgiou, and L. Sakelliou, "On the implementation of a recently proposed dosimetric formalism to a robotic radiosurgery system," Med. Phys. **37**, 2369–2379 (2010).
[15]H. Bouchard, J. Seuntjens, J. F. Carrier, and I. Kawrakow, "Ionization chamber gradient effects in nonstandard beam configurations," Med. Phys. **36**, 4654–4663 (2009).
[16]H. Bouchard, J. Seuntjens, and I. Kawrakow, "A Monte Carlo method to evaluate the impact of positioning errors on detector response and quality correction factors in nonstandard beams," Phys. Med. Biol. **56**, 2617–2634 (2011).
[17]A. J. Scott, A. E. Nahum, and J. D. Fenwick, "Using a Monte Carlo model to predict dosimetric properties of small radiotherapy photon fields," Med. Phys. **35**, 4671–4684 (2008).
[18]R. Alfonso, P. Andreo, R. Capote, M. S. Huq, W. Kilby, P. Kjall, T. R. Mackie, H. Palmans, K. Rosser, J. Seuntjens, W. Ullrich, and S. Vatnitsky, "A new formalism for reference dosimetry of small and nonstandard fields," Med. Phys. **35**, 5179–5186 (2008).
[19]G. Cranmer-Sargison, S. Weston, J. A. Evans, N. P. Sidhu, and D. I. Thwaites, "Implementing a newly proposed Monte Carlo based small field dosimetry formalism for a comprehensive set of diode detectors," Med. Phys. **38**, 6592–6602 (2011).
[20]P. Francescon, W. Kilby, N. Satariano, and S. Cora, "Measurement corrections for output factor measurements of small robotic radiosurgery beams formed by a variable aperture collimator," *Proceedings of the International Symposium on Standards, Applications and Quality Assurance in Medical Radiation Dosimetry (IDOS), Vienna, 9-12 November 2010* (IAEA, Vienna, Austria, 2011), Vol. 1, pp. 181–92.
[21]D. M. Gonzalez-Castano, L. B. Gonzalez, M. A. Gago-Arias, J. Pardo-Montero, F. Gomez, V. Luna-Vega, M. Sanchez, and R. Lobato, "A convolution model for obtaining the response of an ionization chamber in static non standard fields," Med. Phys. **39**, 482–491 (2012).
[22]I. Kawrakow, "Accurate condensed history Monte Carlo simulation of electron transport. II. Application to ion chamber response simulations," Med. Phys. **27**, 499–513 (2000).
[23]I. Kawrakow, "Accurate condensed history Monte Carlo simulation of electron transport. I. EGSnrc, the new EGS4 version," Med. Phys. **27**, 485–498 (2000).
[24]A. J. Scott, A. E. Nahum, and J. D. Fenwick, "Monte Carlo modeling of small photon fields: Quantifying the impact of focal spot size on source occlusion and output factors, and exploring miniphantom design for small-field measurements," Med. Phys. **36**, 3132–3144 (2009).
[25]J. Wulff, J. T. Heverhagen, K. Zink, and I. Kawrakow, "Investigation of systematic uncertainties in Monte Carlo-calculated beam quality correction factors," Phys. Med. Biol. **55**, 4481–4493 (2010).
[26]W. Kilby, J. R. Dooley, G. Kuduvalli, S. Sayeh, and C. R. Maurer, Jr., "The CyberKnife robotic radiosurgery system in 2010," Technol. Cancer Res. Treat. **9**, 433–452 (2010).
[27]C. Antypas and E. Pantelis, "Performance evaluation of a CyberKnife G4 image-guided robotic stereotactic radiosurgery system," Phys. Med. Biol. **53**, 4697–4718 (2008).
[28]G. G. Echner, W. Kilby, M. Lee, E. Earnst, S. Sayeh, A. Schlaefer, B. Rhein, J. R. Dooley, C. Lang, O. Blanck, E. Lessard, C. R. Maurer, Jr., and W. Schlegel, "The design, physical properties and clinical utility of an iris collimator for robotic radiosurgery," Phys. Med. Biol. **54**, 5359–5380 (2009).
[29]W. R. Leo, *Techniques for Nuclear and Particle Physics Experiments: A How-to Approach*, 2nd rev. ed. (Springer-Verlag, 1994).
[30]International Organization for Standarization, *Guide to the Expression of Uncertainty in Measurement (GUM)* (ISO, Geneva, Switzerland, 1995).
[31]P. Castro, F. Garcia-Vicente, C. Minguez, A. Floriano, D. Sevilliano, L. Perez, and J. J. Torres, "Study of the uncertainty in the determination of the absorbed dose to water during external beam radiotherapy calibration," J. Appl. Clin. Med. Phys. **9**, 70–86 (2007).
[32]P. Sharpe and J. Sephton, "Therapy level alanine dosimetry at the NPL," in *Proceedings of the 216th PTB Seminar: Alanine Dosimetry for Clinical Applications*, Braunschweig, Germany (PTB, Braunschweig, Germany, 2006).
[33]S. Devic, J. Seuntjens, E. Sham, E. B. Podgorsak, C. R. Schmidtlein, A. S. Kirov, and C. G. Soares, "Precise radiochromic film dosimetry using a flat-bed document scanner," Med. Phys. **32**, 2245–2253 (2005).
[34]L. Petrokokkinos, M. Kozicki, E. Pantelis, C. Antypas, J. Fijuth, P. Karaiskos, L. Sakelliou, and I. Seimenis, "Characterization of a new polymer gel for radiosurgery dosimetry using magnetic resonance imaging," J. Instrum. **4**, P06018 (2009).
[35]L. Petrokokkinos, K. Zourari, E. Pantelis, A. Moutsatsos, P. Karaiskos, L. Sakelliou, I. Seimenis, E. Georgiou, and P. Papagiannis, "Dosimetric accuracy of a deterministic radiation transport based ^{192}Ir brachytherapy treatment planning system. Part II: Monte Carlo and experimental verification of a multiple source dwell position plan employing a shielded applicator," Med. Phys. **38**, 1981–1992 (2011).
[36]Y. De Deene, R. Van de Walle, E. Achten, and C. De Wagter, "Mathematical analysis and experimental investigation of noise in quantitative magnetic resonance imaging applied in polymer gel dosimetry," Signal Process. **70**, 85–101 (1998).
[37]P. Francescon, W. Kilby, N. Satariano, and S. Cora, "Monte Carlo simulated correction factors for machine specific reference field dose calibration and output factor measurement using fixed and iris collimators on the CyberKnife system," Phys. Med. Biol. **57**, 3741–3758 (2012).